Onsite treatment of wastes in municipal waste incinerator: Co-sintering of fly ash and leachate sludge into value-added ceramic granule

Yujie Xue [a], Xiaochen Lin [b], Houhu Zhang [b], Dong Zou [a], Jizhi Zhou [a,*], Yufeng Zhang [a,**]

[a] School of Environmental Science and Engineering, Nanjing Tech University, No. 30 Puzhunan Road, Jiangsu, 211816, PR China
[b] Nanjing Institute of Environmental Sciences, Ministry of Ecology and Environment of the People's Republic of China, Nanjing, 210042, PR China

A R T I C L E   I N F O

A B S T R A C T

The leachate sludge (LS) and fly ash (FA) are the foci of hazardous wastes which generated from the municipal solid waste incineration (MSWI). The current work developed a new way to use energy from MSWI process for the on-site sintering of LS and FA at a relatively low temperature. With the assistance of CaF_2, granule of LS and MSWI FA were co-sintered. The influence of temperature, the mass of CaF_2, and the mass ratio of LS/MSWI FA were investigated. As a result, heavy metals volatilization and leaching in the form of chlorinated salts were controlled. In addition, CaF_2 improved the compressive strength of the granule under low-temperature sintering. Moreover, the scale-up co-sintering test was achieved in an MSWI chamber. The results showed that the optimum condition was sintering at 973K for 1 h. The compressive strength of sintered product reached 4.25 MPa, which met the standard of ceramic granule. Moreover, with the addition of CaF_2, the volatilization rate of Pb, Zn, and Cd decreased by 6%, 7%, and 6%, respectively. This method can be a promising technique for the utilization of solid wastes.

1. Introduction

Incineration, a prevalent approach to treat municipal solid waste (MSW) before landfilling, provides a volume reduction of up to 90%, destruction of pathogenic agents, and enables potential energy recovery. However, incineration inevitably produces large amounts of fly ash (FA), and remains risky for secondary pollution. For instance, every year, China produces approximately 6.15 kg of MSWI FA per inhabitant, in which South Korea produces 2.92 kg MSWI FA per inhabitant, Japan produces 7.68 kg MSWI FA per inhabitant, UK produces 5.39 kg MSWI FA per inhabitant. On the other hand, MSWI FA is a problematic residue with high chloride content, and significant amounts of heavy metals (lead, zinc, etc.) [1,2]. Shi et al. studied the environmental and human health risk of FA [3]. Consequently, the effective treatment of FA is a hot issue. MSWI FA is classified as hazardous waste and must be treated with caution and specificity. On the other hand, incineration plants also produce approximately 30 tons/day of leachate sludge (LS), also known as the solid waste produced during the treatment of landfill leachate in typical domestic waste incineration plants. Due to the large amount and complex composition, it is of great importance that LS be properly handled to minimize the hazard as well as the

---

secondary pollution, i.e., the escape of heavy metals contents.

The stabilization treatment of heavy metals in wastes has been largely investigated, such as the thermal process, three-dimensional electrokinetic method, immobilization method, and plasma vitrification technologies [4–13]. Toward conversion into value-added products, some researchers studied the construction application of FA and its derivatives, such as glass-ceramics and concrete, which is potentially beneficial for the environment and economy [14–19]. Among the technologies for FA utilization, high-temperature sintering is the current mainstream treatment, which can improve the stabilization of heavy metals in MSWI FA. In regards to the volatilization of heavy metals in the FA, Binbin Li et al. studied the temperature effect on heavy metals volatilization and concluded that the volatilization rate increased with the increase in temperature [20]. Jie Yu et al. studied the mechanism of heavy metals vaporization from MSWI FA [21]. Zhenrong Zhang et al. studied the effect of CaO on heavy metals volatilization and concluded that CaO decreased the volatilization efficiency of Cr and Cu [22]. Besides, the higher water content of leachate may also cause difficulties during disposal. One widely used technique to reduce the volume and mass of LS is the combustion, which could lead to 39% residue in the total mass of LS. Xingrun Wang et al. characterized the sintered product at temperatures in the range of 1293–1323K, and the concentration of heavy metals in the leachate was found to be in the range of China's regulatory requirements [23].

MSWI FA and LS contain SiO_2, Al_2O_3, and Fe_2O_3, these substances are the main ingredients of ceramsite. Consequently, co-sintering is promising for ceramic production. Currently, lightweight aggregate is mainly manufactured through sintering of natural materials including shale, clay, perlite, etc. Considering the ability of removal and stabilization of pollutants during the high temperature sintering process, there is a growing concern on recycling of waste materials for production of lightweight aggregate. Numerous literatures had applied this technology on municipal sludge, fly ash, coal fly ash, sewage sludge, etc [24–28]. Xingrun Wang et al. successfully manufactured lightweight aggregate from sewage sludge and coal ash, and the concentration of heavy metals ranged well within the limit of China's regulatory requirements [29]. Xingwen Lu et al. studied the immobilization of Zn and Pb in Pb–Zn sludge into $Zn(Al_{0.5}Fe_{1.5})O_4$ and $Ca_{5.5}Pb_{4.5}(PO_4)_6(OH)_2$ structures by thermal treatment with sewage sludge ash. Overall, 87% of Pb and 98.7% of Zn in sludge were transformed to $Ca_{5.5}Pb_{4.5}(PO_4)_6(OH)_2$ and $Zn(Al_{0.5}Fe_{1.5})O_4$ at 1000 °C after 3 h of sintering [30]. The heavy metals leaching concentration of sintered products met the requirement of standard by sintering in the previous study [31–33]. Some researchers have measured the properties of ceramic produced from the co-sintering of FA and sludge, the products meet the requirement of ceramistes [34–38]. Changyong Li demonstrated that the compressive strength of lightweight aggregate was no less than 3 MPa produced from sintered sludge [34]. Fanlu Min demonstrated that the compressive strength of the sintered products reached higher than 8 MPa by co-sintering of FA and municipal sludge 1223K–1423K [36]. Guanhua Jia concluded that the compressive strength reached 5.11–7.86 MPa with the sintering temperature of 1473K–1523K [37]. Glory Joseph fabricated aggregate concrete with fly ash and the compressive strength reached 45 MPa [39]. Wael Zatar1 and Tu Nguyen studied fiber-reinforced self-compacting concrete production with the replacement of fly ash and concluded that the maximum three-day compressive strength was 43 MPa [40]. According to the previous study, FA co-sintering with other wastes could produce ceramic granule and stabilize heavy metals. These cases suggest a high -temperature sintering for fly ash stabilization. Moreover, the heavy metal chloride is more likely to volatilization at high temperature [41]. Fortunately, it had been reported that certain sintering additives could decrease the melting point of sample. For instance, Ying Zhou et al. studied melanotekite structure to stabilize heavy metals under lower temperature [42]. Shao-Hua Hu et al. demonstrated the addition of Na_2CO_3 could decrease the sintering temperature of the mixture [43]. Liang Wang et al. demonstrated that clay sludge could decrease the melting point of waste [44]. It is expected that during the incineration of MSWI FA and LS, CaF_2 could be a promising additive to adjust the temperature and activate the co-sintering, as well as to tune the process pathways towards desired products (e.g., ceramsite).

Herein, a co-sintering strategy of MSWI FA and LS had been proposed, it introduced CaF_2 into the system and a series of assessments were carried out to investigate the influence of sintering temperature, heavy metal volatilization, as well as the compressive strength of the value-added product. It was expected that the CaF_2 would significantly lower the sintering temperature and decrease the heavy metals volatilization, indicating that this approach could effectively reduce energy consumption. We also test the process in a pilot chamber, indicating the good scalability of this technique. The process was also designed to be energy-efficient as it would only rely on the internal incineration heat from the facility. The study aimed to establish an on-the-spot treatment strategy with high waste-to-raw material conversion, which could be promising for future MSW treatment.

2. Materials and methods

2.1. Materials

The MSWI FA used in this study was collected from the incineration air pollution control system in the municipal waste incinerator in Shanghai, China. The leachate sludge was collected in the treatment process of leachate in the same facility, which was from the municipal solid waste storage.

Element analysis of FA and LS was performed by X-ray fluorescence spectroscopy (XRF-1800, Japan SHIMADZU LIMITED). As shown in Table S1 , the major components of MSWI FA were CaO, Cl, Na_2O, SiO_2, and Al_2O_3. It is worth mentioning that chloride salts were important parts of MSWI FA, and Cl constituted 31.64% by weight. In addition, LS contained CaO, Al_2O_3, Fe_2O_3, and SiO_2 as the main compositions. Besides, hazardous heavy metals of MSWI FA and LS including zinc (Zn), lead (Pb), copper (Cu), chromium (Cr), nickel (Ni) and cadmium (Cd) are also present as shown in Table S2. The MSWI FA leaching concentration of Zn and Cd were higher than that in the regulation limitation for hazardous materials. The same situation was observed in the case of LS in which the leaching concentration of Pb and Cr exceeded the regulation limitation.

2.2. A laboratory-scale treatment

A laboratory-scale treatment was selected to ensure that various experimental parameters could be well investigated. The treatment process included raw material preparation, mixing, pelletization, drying, sintering, and cooling.

2.2.1. Mixing and pelletization

At room temperature, 260.0 g of raw MSWI FA and 200 g of LS were mixed and the resulting sample was denoted as sample A. Then various mass of CaF_2 (4.6 g, 9.2 g, 13.8 g and 18.4 g) were added, and the resulting samples were named as sample B1, B2, B3 and B4, respectively. All mixtures in five beakers were stirred for 30 min, followed by a manually granulation process at room temperature. All pellet samples were 10 mm–20mm diameter in size. The granule sample A, made of 260.00 g of raw MSWI FA and 200.00 g of LS, was set as the control.

2.2.2. Drying

After being made into pellets, all samples were dried in a drying oven (DHG-9075A drying oven, Shanghai Yiheng Technology Co., LTD) at 353K for 24 h to regulate the moisture content.

2.2.3. Sintering

The optimal temperature was determined as follows. In all experiments, the feeding temperature was set as the ambient temperature. The raw aggregate pellets experienced a temperature increase, both internally and externally, during sintering. Raw aggregate pellets were heated to 773, 873, 973, and 1073K and sintered for 30, 60, 90, and 120 min in Muffle Furnace (SX-G12123 Muffle Furnace, Tianjin Zhonghuan Experimental Electric Furnace Co., LTD), respectively.

2.2.4. Cooling

The sintered pellets were naturally cooled to room temperature in this study.

2.3. The co-sintering treatment in MSWI facility

Similar procedures were also carried out at a pilot scale. Specifically, at room temperature, 5 tons of raw MSWI fly and 1 ton of LS were mixed for the extrusion granulation, which provided more compact granule than that in laboratory test and was achieved by the industrial equipment. Then stirring 15 min every time for six times. The total particles were packed in six bags and every bag was 1 ton. The particles were sintered at 873–973K, the feeding rate was 1 ton/h.

2.4. Characterizations and analyses

2.4.1. Toxicity characteristic leaching procedure (TCLP) test

The leaching concentration of heavy metals was conducted according to US-EPA SW 846 TCLP test method 1311. The particles were put in centrifuge tube with the liquid solid ratio 20:1. Then the mixtures were shaken for 18 h on a reciprocal shaker (FZ-4 Flip shaker, Changzhou Jintan Boke Test Equipment Research Institute) at the speed of 30 rpm, followed by the centrifuge for 10 min at the speed of 3000 rpm. Ultimately, the liquid was filtered by 0.45 μm filter membrane. The heavy metals ion concentration in liquid were detected by inductively coupled plasma-atomic emission spectrometry (ICP-AES, Leeman Instrument Co., LTD).

2.4.2. X-ray diffraction (XRD) analysis

The mineral phases of samples were identified via XRD measurement. The XRD analysis was performed on a Rigaku DLMAX-2550 XRD using MDI Jade 5.0 software (Materials Data Inc, Liverpool, CA). Measurement was carried out with a Cu target (Kα, λ = 0.154 nm). The scanning rate was set as 5°/min and the scanning angle range (2 theta) was from 10° to 80°.

2.4.3. Heavy metal content test

Heavy metals in raw samples and the sintered samples were extracted by microwave-assisted acid digestion (HNO_3/HF). The samples were put in the polytetrafluoroethylene beaker with the HNO_3/HF ratio 2:1. The mixture of samples and acids was uniformly placed in the microwave oven for 60 min for digestion. Then the mixture was cooled and poured into the glass crucible, and then electrically heated to evaporate the HF to obtain the nitric acid solution of heavy metals. The remaining liquid sample was diluted to 50 mL with deionized water. The liquid sample was filtered by 0.45 μm filter membrane. Finally, the heavy metals concentration was measured by (ICP-AES, Leeman Instrument Co., LTD).

2.4.4. Compressive strength test

Compressive strength of the ceramic granules was measured at a loading rate of 1 mm/min using a universal material testing machine (AG-IC 20 KN, Shimadzu, Japan). For each sample, five specimens were measured to obtain the mean value and standard deviation.

3. Results and discussion

3.1. Effect of moisture content

Fig. 1 showed the moisture content of different FA/LS ratios. The moisture content of the mixture decreased with the increase in the FA/LS ratio. The particles at the FA/LS ratio of 1:1, 1.1:1, and 1.2:1 had high moisture content, which were difficult to form stable pellets. However, the moisture contents of the particles at the FA/LS ratio of 1.4:1 and 1.5:1 were low, which were easy to break in the feeding process. The particle moisture content of the 1.3:1 mixture was moderate. The texture was compact and not easy to crack. Consequently, 1.3:1 was chosen for the optimal FA/LS ratio in the laboratory-scale treatment.

Table 1 showed the element contents with the FA/LS ratio of 1.3:1. The FA/LS ratio of 1.3:1 sample had a relatively high content of Zn, Pb, Cd、Cu, Cr and Ni. Compared with FA, the concentration of Zn、Pb、Cu and Cd decreased in the mixture. Compared with LS, the concentration of Cr and Ni decreased in the mixture. The major element of the FA/LS ratio of the 1.3:1 sample was 31.16% of Ca, 28.04% of O and 19.29% of Cl, respectively.

3.2. Effect of sintering duration and temperature

In all experiments, the feeding temperature was set as ambient temperature. The raw aggregate pellets experienced a temperature increase both internally and externally during sintering. Fig. 2 showed the compressive strength of sintered products at different temperatures and for different durations. The obtained products demonstrated a compressive strength ranging from 0.25 to 4.25 MPa. It was also seen that the compressive strength was the lowest when sintering temperature performed at 773K, the reason could be that such a short duration probably did not allow the reaction to complete and the substances in the products were not fully bonded. Hence, the sintered products had a compressive strength of only 0.25–0.4 MPa, which were approximated to raw aggregate pellets. And the compressive strength was the highest when sintering temperature performed at 973K for 60min. The compressive strength increased with the increment of sintering temperature when the sintering temperature was lower than 973K and sintering duration was lower than 120 min. However, the 30 min sintering did not result in a stable granule as the compressive strength decreased to 2.5 MPa when the temperature rose to 1073K. It may be relative to the crack of sample at high temperature with high moisture content, which led to much water evaporation within a short time. On the contrary, the compressive strength was the lowest at 973K when the sintering duration for 120min. Sintering duration had an impact effect on the compressive strength. With the increase of sintering duration, the compressive strength increased to 4.25 MPa at 973K, then decreased when the sintering duration exceeded 60 min.

It proposes that the sintering temperature and duration played a significant role in determining the compressive strength of the sintered products. Consequently, the appropriate condition was 973K and 60min.

3.3. Effect of CaF$_2$

Fig. 3 showed the compressive strength of sintered products sintered at different temperatures and different CaF$_2$ additions for 1 h. The compressive strength was the lowest when sintering was performed at 773K, consistent with the result shown in Fig. 2. The highest compressive strength of 6.35 MPa can be achieved by sintering at 1073K for 60min. We also observed that the curves of sample A and sample B1 were close to each other, the rest of the curves were significantly higher, especially the curve of sample B2. Based on the results above, it can be concluded that CaF$_2$ can obviously improve the compressive strength of sintered products, and the most suitable addition was 9.2g CaF$_2$.

As shown in Fig. 4(a), the mass loss of sample A was recorded by TG curve, which showed a 7.3% decline of mass before 973K,
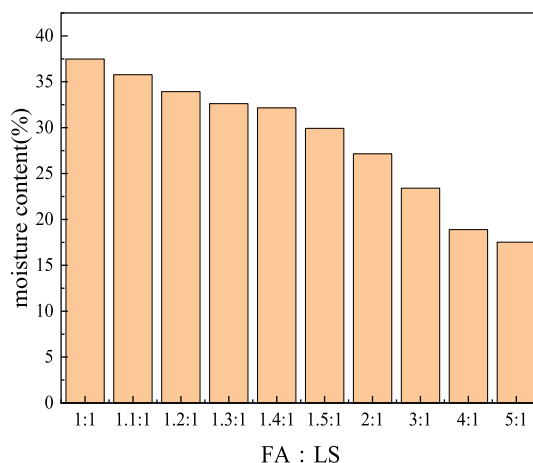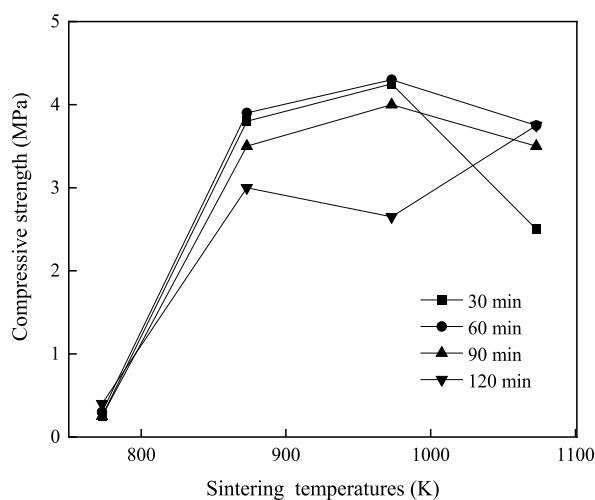

Fig. 1. Moisture content of different FA/LS ration.

Table 1
The content of heavy metals and element with the ratio of 1.3:1.

Heavy metals	Concentration(mg/kg)	Element	Mass(%)
Zn	5194.39	O	28.04
Pb	1055.69	Ca	31.16
Cd	95.65	C	7.09
Cu	591.13	Al	2.49
Cr	283.21	Fe	2.58
Ni	146.82	Si	1.72
		Mg	0.9
		P	0.68
		Na	2.86
		Cl	19.29
		S	1.91
		Zn	0.67

Fig. 2. Relationship between sintering duration and compressive strength at different sintering temperatures.
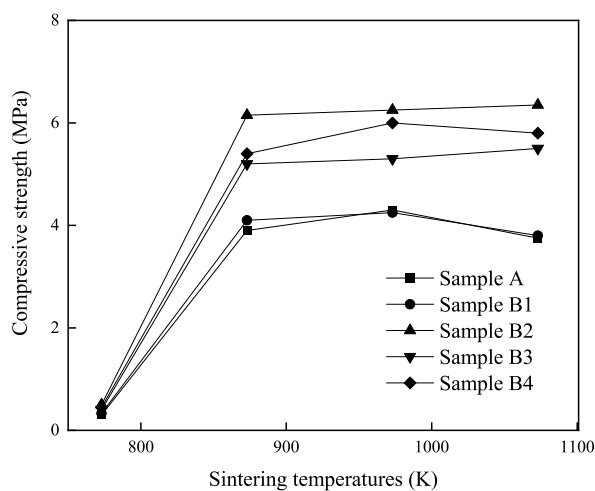
Fig. 3. Compressive strength comparison of raw sintered pellets and CaF$_2$-pretreated sintered pellets.

followed by 11% loss of mass at 973–1073K. The corresponding DTA curve showed a broad endothermic peak at 773K, which could be assigned as dehydration of hydroxyl compounds such as Ca(OH)$_2$ [45]. The endothermic peak after 1023K might reflect the heavy metals chloride salt volatilization as the mass loss at 973–1073 K. In comparison, the similar mass losses of sample B2 were shown in Fig. 4(b), which recorded a mass loss of 8.53% before 973K and 11.4% at 973–1073K. The broad endothermic peak was shown at 723K
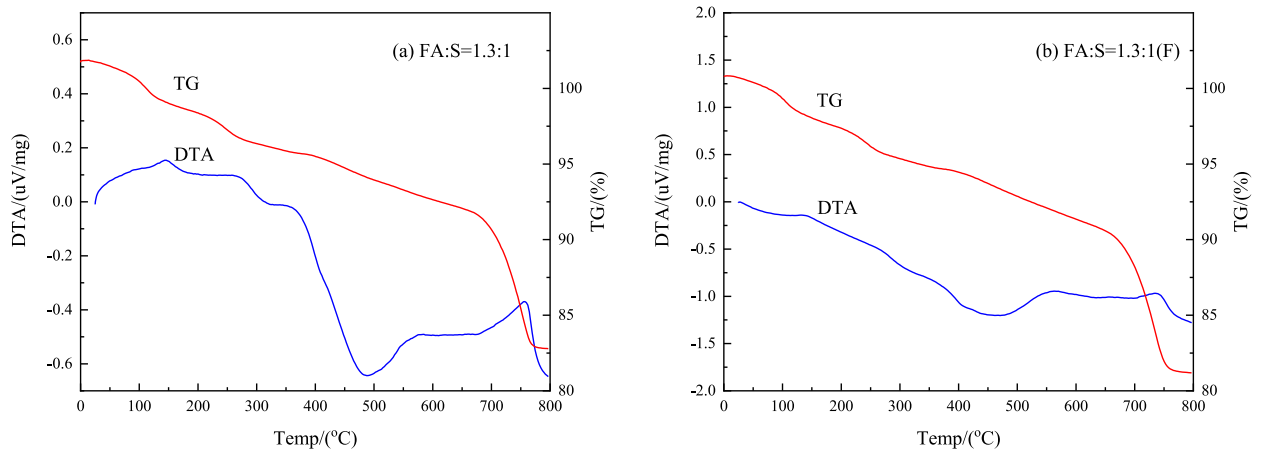
Fig. 4. TG/DTA curves of (a) sample A and (b) sample B2 heating at 273–1073K in air at a rate of 4°/min.

with the endothermic peak after 1023K were associating well with the observation from sample A. The result showed that the mass loss rate of sample B2 was faster than that of sample An under the same heating program, probably because of the addition of CaF₂, which decreased the sintering temperature and accelerated reaction process. Comparing the quality loss between the two temperatures, it can be found that substantial weight loss occurred at 973K and above, indicating that 973K could be essential for the desired temperature.

3.4. Heavy metals residues and volatilization rate in the sintered samples

The heavy metals concentration in the samples after sintering were measured and the results were shown in Table 2. It showed that heavy metals concentration decreased with the increase in sintering temperatures. It can also be observed that the overall heavy metals concentration in sample A were higher than the heavy metals concentration in sample B2.

The heavy metals in the mixed system of MSWI FA and leachate sludge volatile at 1073K as the result of the Cl with high content in MSWI FA was transformed into heavy metals chloride with a low boiling point. The volatilization rate (γ_1, %) of heavy metals was calculated to analyze the effect of sintering temperature on the volatilization rate of heavy metals in two samples, and expressed as the following equations.

$$\alpha_1 = \frac{10 - m_1}{10} \times 100\% \tag{Eq. 1}$$

$$\beta_1 = \frac{Q}{1 - \alpha_1} \times E \tag{Eq. 2}$$

$$\gamma_1 = \frac{\beta_1 - QW}{\beta_1} \times 100\% \tag{Eq. 3}$$

α_1 (%) is the rate of mass loss after sintering; m_1 is the mass of sample after sintering, 10 is the mass of sample before sintering, β_1 (kg)is the mass of heavy metals before sintering, Q (kg) is the mass of sintered sample, E (mg/kg) is the heavy metals concentration before sintering, W (mg/kg) is heavy metals concentration after sintering, γ_1(%) is the volatilization rate.

Fig. 5 showed the volatilization rate of the main heavy metals (Pb, Zn, and Cd) in FA and LS. As can be seen, the volatilization rate of

Table 2
Total concentration of heavy metals in the sintered samples.

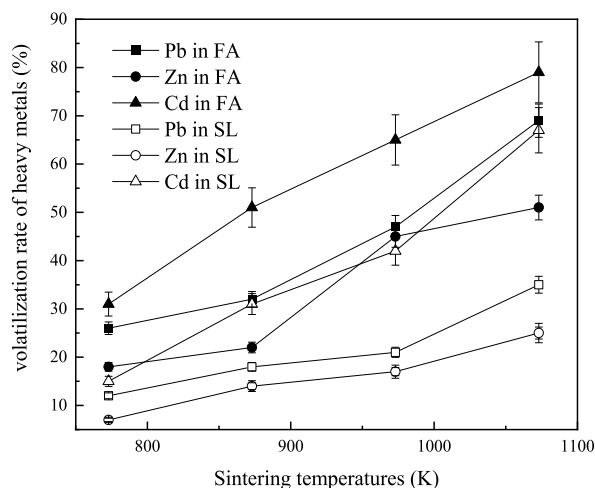| Sintering temperature (K)	Total concentration (mg/kg)		
	Pb	Zn	Cd
sample A			
773	1680	6400	130
873	1575	6000	117
973	1550	5800	105
1073	1400	5300	75
sample B2			
773	1570	6000	115
873	1360	5150	100
973	1300	4300	84
1073	1200	3300	62

Fig. 5. Volatilization characteristic comparison of main heavy metals from FA and LS.

heavy metals in MSWI FA and LS gradually increased with the increase in temperature. And the volatilization rate of Pb 、 Zn and Cd in MSWI FA was generally higher than that of LS, which could be induced by the larger amount of chlorine in MSWI FA. The volatilization characteristic comparison of the primary heavy metals (Pb, Zn, and Cd) in sample A and sample B2 were presented in Fig. 6. It showed that γ_1 values increased with the increase of sintering temperature. Cd was the most vaporizable metal (40% at 773K, 82% at 1073K), followed by Pb (36% at 773K, 70% at 1073K) and by Zn (3% at 773K, 58% at 1073K). Obviously, the highest volatilization rate of these heavy metals occurred at 1073K. The volatilization rate of these heavy metals in sample An under 1073K were much higher than that of sample B2. The result showed that the addition of CaF$_2$ effectively reduced the volatilization rate of heavy metals, suggesting that CaF$_2$ probably decreased the melting point of the mixture and partial melt stabilizes heavy metals.

3.5. Chemical properties of sintered products

In order to evaluate the release of heavy metals in environmental conditions, a leaching test modified from US EPA TCLP Method 1311was used to investigate the leaching concentration of heavy metals from the sintered samples. Table 3 showed the TCLP results of the sintered pellets manufactured in this study. As can be seen, ranging from 773 to 1073K, the higher the sintering temperature, the smaller the amount of heavy metals leached except Pb. As sintering temperature exceeded 973K, only trace amounts of Zn, Pb, Cd and Cr were detected but not Ni and Cu in sample A. In addition, the leaching concentration of Zn、Cr、Pb and Cd decreased when adding CaF$_2$ into samples, implying that the sintered products fabricated were potentially non-hazardous for construction use. The values were compared with the regulatory standard limits required by the Chinese National standard GB 5085.3–2007. The results indicated that all the values were much lower than regulatory standard limits and suggested a low leaching risk of heavy metals from the sintered samples.
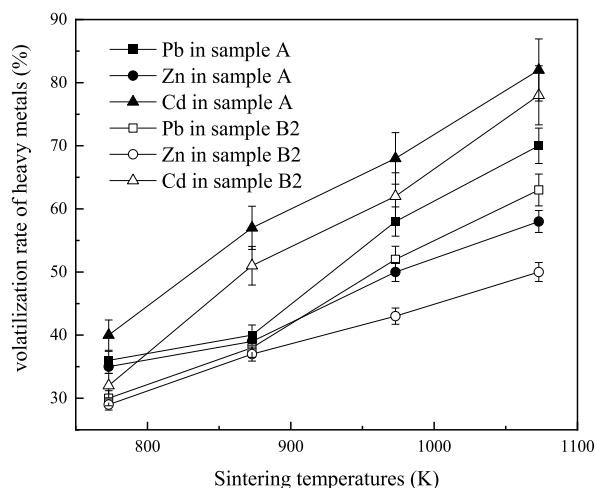

Fig. 6. Volatilization characteristic comparison of main heavy metals from sample A and sample B2.

Table 3
Leaching concentration of heavy metals.

Sintering temperature (K)	Leaching concentration (mg/L)					
	Ni	Cu	Zn	Cr	Cd	Pb
sample A						
773	–	–	0.22	0.39	0.21	–
873	–	–	0.22	0.42	0.19	–
973	–	–	0.06	0.33	0.18	–
1073	–	–	0.04	0.24	0.18	0.26
sample B2						
773						
873	–	0.82	0.12	0.08	0.12	–
973	–	0.43	0.03	0.04	–	–
1073	–	–	–	0.02	–	–
Toxicity threshold						
	5	100	100	15	1	5

- represents undetected.

3.6. Sintering process and stability of heavy metal

The MSWI FA and LS were determined as a weight ratio of 1.3:1. Ternary phase diagram (Fig. 7) showed the melting points of industrial glass with various contents of Al_2O_3, SiO_2, and CaO. It was noted that the low melting point of the solid mixture was relative to the high Si content with a proper mass ratio of CaO and Al_2O_3. The content of CaO was higher than LS, indicating that the melting point of FA was higher than 2673K. Therefore, the energy consumption of melting FA or LS may be very high. To make the process more environment-friendly, it is necessary to add auxiliary materials to reduce the melting point. With the increase ratio of auxiliary materials, the sample in the three-phase diagram gradually moved towards the upper right, from the high melting point area to the low melting point area.

Compared with the sintering temperature of previous study, the sintering temperature was above 1123K.However, the sintering temperature of the current work was lower than 1073K. This was contributed by the ratio of FA and LS, as well as the Al_2O_3 and SiO_2 contents, which could decrease the melting point. With the increase of auxiliary materials ratio, the melting effect improved, and the concentration of heavy metals decreased. The concentration of heavy metals decreased when the sample melted completely as the result of the vitreum formed by the melting process could stabilize heavy metals. The increase of vitreum content was conducive to the stabilization of heavy metals.

Table 4 showed the mass balance of heavy metals during the sintering process. The mass of Pb, Zn, Cd in the sintering product reached 910 mg,3010 mg,58.8 mg at the temperature of 973K. The Pb concentration of 1.3:1 mixture was 1055.69 mg/kg, which was approximate to 1099 mg/kg at 773K. The mass loss of the sample was high at 973K, it is probably caused by the decomposition of organic matter in the LS during the sintering process, which led to the content change of heavy metals.

Fig. 8 showed the XRD patterns of MSWI FA and LS. The main crystalline phases were presented in FA include calcium carbonate ($CaCO_3$), anhydrous gypsum ($CaSO_4$), potassium chloride (KCl) and sodium chloride (NaCl). The peaks of NaCl and $CaCO_3$ phases were obvious and strong. The large amounts of $CaCO_3$ in the FA may had been derived from the CaO carbonation reaction. Furthermore, the CaO reacted with SO_3 to form $CaSO_4$. Most Cl components in the FA existed in the form of soluble salts, such as NaCl and KCl. On the other hand, the main crystalline phases in LS are SiO_2 and $CaCO_3$.

The XRD patterns of two kinds of samples sintered at 973K for 1 h were recorded in Fig. 9. Compared to the original sample, calcium chloroaluminate phase ($Ca_{12}Al_{14}O_{32}Cl_2$) was formed in samples sintered at 973K for 1 h. The result of XRD analysis showed the disappearance of sodium chloride (NaCl) in sintered sample B. There were still peaks of potassium chloride (KCl), and calcium carbonate ($CaCO_3$). The reason could be expressed as calcium carbonate was hard to be decomposed under 973K, and the chlorine was not completely evaporated. According to the mineral phases formed in this sintering process, indicating that heavy metals stabilized in the sintered products. The result of the XRD analysis also showed that the formation of $Ca_5(PO_4)_3(OH)$ in sintered sample A.

In the co-sintering process, the easily fused material gives priority to the formation of amorphous vitreous. During the co-sintering process, Al_2O_3 and CaF_2 formed into new phases. Heavy metals stabilized into new amorphous vitreous. Ca–Al–Si structure was the common structure in the previous study, for instance, aluminosilicates, $Ca_3Al_2O_6$, $Na_{12}Al_2Si_{12}O_{48}(H_2O)_{27}$ [27]. However, the amorphous vitreous of sample B was calcium chloroaluminate because of the lower content of Si in the FA/LS mixture.

3.7. Scale-up test

In fact, the laboratory scale and pilot scale adopted different granulation methods, which the different moisture of sample was required. In the laboratory scale, the properties of 1.3:1 pellets had high water content and suitable for manually granulation. On the contrary, the ration of 1.3:1 was not suitable for extrusion granulation. Extrusion granulation has the advantage of higher compressive strength and mass production. The ration of 2:1、3:1、4:1、5:1 was appropriate for extrusion granulation and the moisture content of 5:1 was lower. Hence, 5 tons to 1 ton was chosen in the pilot scale test.

Similar procedures were also carried out at a pilot scale. Specifically, at room temperature, 5 tons of raw MSWI fly and 1 ton of LS
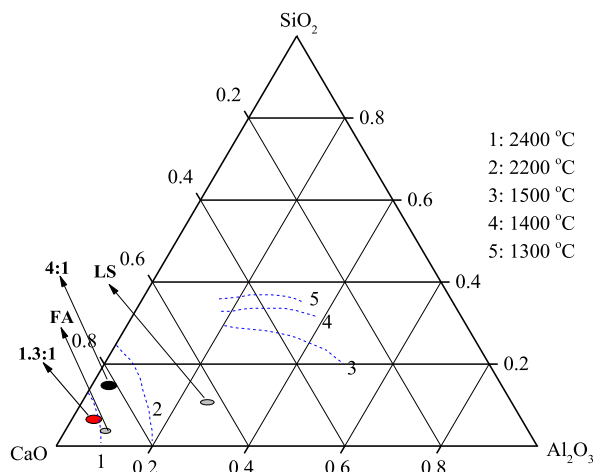
Fig. 7. The region of admixture in the SiO_2–Al_2O_3–CaO ternary plot.

Table 4
Mass balance of heavy metals during the sintering process.

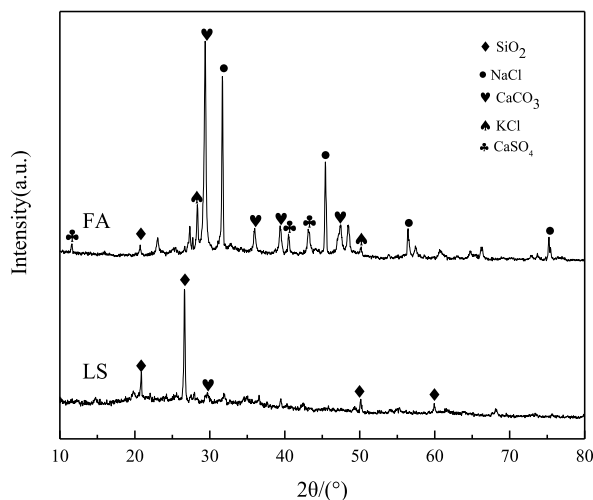|	Temperature(K)	Initial sample(mg)	Product(mg)	Gas(mg)
Pb	773	1508.13	1099	229.08
	873	1508.13	952	288.2
	973	1508.13	910	391.66
	1073	1508.13	840	509.9
Zn	773	7420.56	4200	1054.46
	873	7420.56	3605	1345.34
	973	7420.56	3010	1708.95
	1073	7420.56	2310	1854.4
Cd	773	136.64	80.5	22.09
	873	136.64	70	36.83
	973	136.64	58.8	44.86
	1073	136.64	43.4	51.56

Fig. 8. XRD analysis of FA and LS.

were mixed for the extrusion granulation, which provided more compact granule than that in laboratory test and was achieved by the industrial equipment. The pelletizer and pellets were shown in Fig. 10. The pellet sintered in the incinerator at 873–973K.

In the pilot experiment of low-temperature sintering, the total amount of heavy metals in mixed slag was generally lower than that of the original slag as shown in Table 5. As shown in Table 6, the Cr concentration of the inorganic salt solution quenching medium
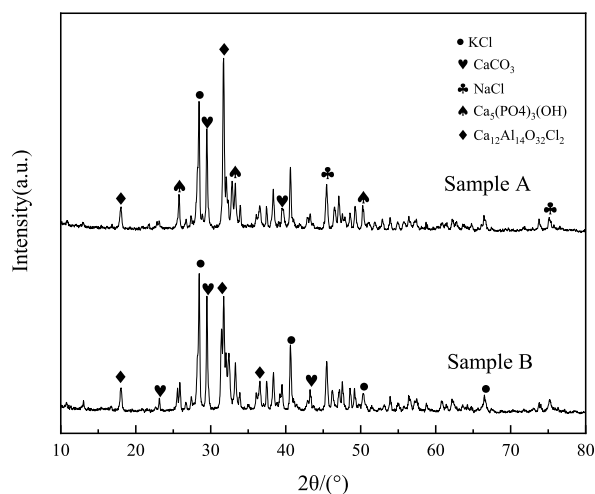
Fig. 9. XRD analysis of sintered sample A and sample B2 (sintering at 973K for 1 h).

Fig. 10. Pelletizer and pellet of scale-up test.

Table 5
Total amount of heavy metals in the mixed slag of lower temperature.

Heavy metals	Original(mg/kg)	Mixed slag(mg/kg)					
		1ton	2ton	3ton	4ton	5ton	6ton
Zn	8541	6167	6034	6123	6342	6183	6213
Pb	832	757	767	743	712	654	633
Cd	–	–	–	–	–	–	–
Cr	2151	1780	1711	1655	1701	1688	1675
Cu	5318	2233	2111	2009	1976	1950	1994
Ni	533	545	566	511	435	457	379

decreased. The heavy metals volatilization rate at lower temperature was lower than that of high temperature as shown in Table 7, which demonstrated that CaF_2 could decrease heavy metals volatilization rate.

As shown in Fig. 11, the mineral phases of raw slag are $Mg_3SiO_4F_2$ and CrF_3.

However, in the mixed slag, the Pb was transformed into new phase $PbHPO_4$. The mixed slag also had $CaCO_3$、Ba_2TiO_4、$BaSiO_4$ phases. The result indicated that heavy metals could be immobilized in the mineral crystal structure, which led to the leaching concentration of heavy metals lower than raw slag.

Table 6

The concentration of heavy metals in the inorganic salt solution quenching medium of lower temperature.

Heavy metals	Origin(mg/L)	Sintered (mg/L)					
		1ton	2ton	3ton	4ton	5ton	6ton
Zn	–	–	–	–	–	–	–
Pb	90	133	121	144	197	202	190
Cd	132	120	134	132	107	56	21
Cr	312	132	111	124	89	68	70
Cu	–	–	–	–	–	–	–
Ni	–	–	–	–	–	–	–

Table 7

The volatilization rate of heavy metals in high/low temperature sintering pilot test.

Heavy metals	volatilization (high temperature)	volatilization (low temperature)
Zn	73.03%	24.99%
Pb	71.95%	33.36%
Cd	75.22%	54.22%
Cr	77.88%	11.92%
Cu	74.06%	55.02%
Ni	74%	16.89%
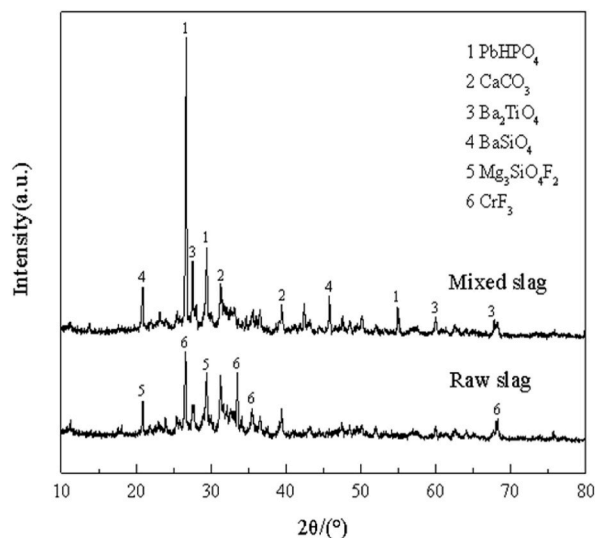
Fig. 11. XRD analysis of low-temperature sintered raw slag and mixed slag.

4. Conclusion

This study developed a novel treatment for MSWI FA and leachate LS, and successfully produced high-intensity pellets through co-sintering. Heavy metals concentration decreased with the increase of sintering temperatures (from 773 to 1073 K). However, the volatilization rate of heavy metals in the sintered samples increased with the increase in sintering temperature. It is found that adding CaF_2 can reduce the heavy metals concentration and volatilization rate in sintered samples significantly. The compressive strength of sintered pellets reached 4.25 MPa. After adding CaF_2, the highest compressive strength of 6.35 MPa can be achieved by sintering at 1073K, which met the requirement of ceramic granule standard.

In the pilot scale test, the total amount of heavy metals in mixed slag decreased, the concentration of Cr and Cd in the inorganic salt solution quenching medium decreased. Compared with laboratory scale experiment, the volatilization rate of Cr decreased above 60%, indicating that pilot scale test is in favor of reduction of heavy metals volatilization rate. Consequently, not only did the process produced useful value-added products, but also proved near-zero discharge.

It is worth mentioning that the strategy highlights a self-supplied energy origin, as the treatment utilized only the internal incineration heat. The zero-waste and energy-efficient treatment was achieved via an on-the-spot cycle, which was well in line with contemporary guidelines. It is complementary to current techniques and will potentially fulfill future needs in pollution management.

Author contribution statement

Yujie Xue: Wrote the paper; Performed the experiments. Xiaochen Lin: Contributed reagents, materials; analysis tools or data. Houhu Zhang: Conceived and designed the experiments. Dong Zou: Analyzed and interpreted the data. Jizhi Zhou: Conceived and designed the experiments. Yufeng Zhang: Conceived and designed the experiments.

Data availability statement

Data will be made available on request.

Declaration of competing interest

The authors declare that they have no known competing financial interests or personal relationships that could have appeared to influence the work reported in this paper.

Appendix A. Supplementary data

Supplementary data to this article can be found online at https://doi.org/10.1016/j.heliyon.2023.e20301.

References

[1] S. Liu, S. Zhao, Z. Liang, F. Wang, F. Sun, D. Chen, Perfluoroalkyl substances (PFASs) in leachate, fly ash, and bottom ash from waste incineration plants: implications for the environmental release of PFAS, Sci. Total Environ. 795 (2021), 148468.

[2] Y. Koike, K. Fujii, R. Saito, N. Ogawa, A. Ohbuchi, Chemical state analysis of heavy metals and radioactive cesium in municipal solid waste incineration fly ash contaminated with radioactive cesium released by the FDNPP accident, Anal. Sci. 37 (2021) 1565–1570.

[3] Y. Shi, Y. Li, X. Yuan, J. Fu, Q. Ma, Q. Wang, Environmental and human health risk evaluation of heavy metals in ceramsites from municipal solid waste incineration fly ash, Environ. Geochem. Health 42 (2020) 3779–3794.

[4] C. Zhao, S. Lin, Y. Zhao, K. Lin, L. Tian, M. Xie, T. Zhou, Comprehensive understanding the transition behaviors and mechanisms of chlorine and metal ions in municipal solid waste incineration fly ash during thermal treatment, Sci. Total Environ. 807 (2022), 150731.

[5] G. Wong, M. Gan, X. Fan, Z. Ji, X. Chen, Z. Wang, Co-disposal of municipal solid waste incineration fly ash and bottom slag: a novel method of low temperature melting treatment, J. Hazard Mater. 408 (2021), 124438.

[6] T. Huang, L. Liu, L. Zhou, K. Yang, Operating optimization for the heavy metal removal from the municipal solid waste incineration fly ashes in the three-dimensional electrokinetics, Chemosphere 204 (2018) 294–302.

[7] E. Atanes, B. Cuesta-Garcia, A. Nieto-Marquez, F. Fernandez-Martinez, A mixed separation-immobilization method for soluble salts removal and stabilization of heavy metals in municipal solid waste incineration fly ash, J. Environ. Manag. 240 (2019) 359–367.

[8] D. Kang, J. Son, Y. Yoo, S. Park, I. Huh, J. Park, Heavy-metal reduction and solidification in municipal solid waste incineration (MSWI) fly ash using water, NaOH, KOH, and NH$_4$OH in combination with CO$_2$ uptake procedure, Chem. Eng. J. 380 (2020), 122534.

[9] P. Chen, H. Zheng, H. Xu, Y. Gao, X. Ding, M. Ma, Microbial induced solidification and stabilization of municipal solid waste incineration fly ash with high alkalinity and heavy metal toxicity, PLoS One 14 (2019), e0223900.

[10] Y. Sun, C. Xu, W. Yang, L. Ma, X. Tian, A. Lin, Evaluation of a mixed chelator as heavy metal stabilizer for municipal solid-waste incineration fly ash: behaviors and mechanisms, J. Chin. Chem. Soc. 66 (2019) 188–196.

[11] X. Zhao, J. Yang, N. Ning, Z. Yang, Chemical stabilization of heavy metals in municipal solid waste incineration fly ash: a review, Environ. Sci. Pollut. Res. Int. 29 (2022) 40384–40402.

[12] S. Pei, T. Chen, S. Pan, Y. Yang, Z. Sun, Y. Li, Addressing environmental sustainability of plasma vitrification technology for stabilization of municipal solid waste incineration fly ash, J. Hazard Mater. 398 (2020), 122959.

[13] W. Ma, W. Shi, Y. Shi, D. Chen, B. Liu, C. Chu, D. Li, Y. Li, G. Chen, Plasma vitrification and heavy metals solidification of MSW and sewage sludge incineration fly ash, J. Hazard Mater. 408 (2021), 124809.

[14] C. Zeng, Y. Lyu, D. Wang, Y. Ju, X. Shang, L. Li, Application of fly ash and slag generated by incineration of municipal solid waste in concrete, Adv. Mater. Sci. Eng. (2020) 1–7.

[15] Y. Huang, J. Chen, S. Shi, B. Li, J. Mo, Q. Tang, Mechanical properties of municipal solid waste incinerator (MSWI) bottom ash as alternatives of subgrade materials, Adv. Civ. Eng. (2020), 9254516.

[16] A. Kanhar, S. Chen, F. Wang, Incineration fly ash and its treatment to possible utilization: a review, Energies 13 (2020) 6681.

[17] M. Irshidat, N. Al-Nuaimi, M. Rabie, Sustainable alkali-activated binders with municipal solid waste incineration ashes as sand or fly ash replacement, J. Mater. Cycles Waste Manag. 24 (2022) 992–1008.

[18] W. Fan, B. Liu, X. Luo, J. Yang, B. Guo, S. Zhang, Production of glass–ceramics using Municipal solid waste incineration fly ash, Rare Met. 38 (2017) 245–251.

[19] Z. Phua, A. Giannis, Z. Dong, G. Lisak, W. Ng, Characteristics of incineration ash for sustainable treatment and reutilization, Environ. Sci. Pollut. Res. Int. 26 (2019), 16974-1699.

[20] B. Li, H. Fan, S. Ding, Y. Luan, Y. Sun, Influence of temperature on characteristics of particulate matter and ecological risk assessment of heavy metals during sewage sludge pyrolysis, Materials 14 (2021) 5838.

[21] J. Yu, L. Sun, C. Ma, Y. Qiao, J. Xiang, S. Hu, H. Yao, Mechanism on heavy metals vaporization from municipal solid waste fly ash by MgCl$_2$6H$_2$, O. Waste Manag 49 (2016) 124–130.

[22] Z. Zhang, Y. Huang, Z. Zhu, M. Yu, L. Gu, X. Wang, Y. Liu, R. Wang, Effect of CaO and montmorillonite additive on heavy metals behavior and environmental risk during sludge combustion, Environ. Pollut. 312 (2022), 120024.

[23] X. Wang, Y. Jin, Z. Wang, Y. Nie, Q. Huang, Q. Wang, Development of lightweight aggregate from dry sewage sludge and coal ash, Waste Manag. 29 (2009), 1330-133.

[24] X. Zhan, L. Wang, L. Wang, J. Gong, X. Wang, X. Song, T. Xu, Co-sintering MSWI fly ash with electrolytic manganese residue and coal fly ash for lightweight ceramisite, Chemosphere 263 (2021), 12791.

[25] K. Lin, K. Lo, J. Shie, B. Tuan, C. Hwang, Y. Chang, Properties and microstructure of eco-cement produced from co-sintered washed fly ash and waste sludge, Environ. Prog. Sustain. Energy 35 (2016) 764–771.

[26] K. Lin, K. Lo, J. Shie, B. Tuan, C. Hwang, Y. Chang, Hydration characteristics of cement for co-sintered from washed-fly ash and waste sludge, Environ. Prog. Sustain. Energy 34 (2015) 964–972.

[27] T. Li, T. Sun, D. Li, Preparation, sintering behavior, and expansion performance of ceramsite filter media from dewatered sewage sludge, coal fly ash, and river sediment, J. Mater. Cycles Waste Manag. 20 (2016) 71–77.

[28] Y. Shao, Y. Shao, W. Zhang, Y. Zhu, T. Dou, L. Chu, Z. Liu, Preparation of municipal solid waste incineration fly ash-based ceramsite and its mechanisms of heavy metal immobilization, Waste Manag. 143 (2022) 54–56.

[29] X. Wang, Y. Jin, Z. Wang, R. Mahar, B.Y. Nie, A research on sintering characteristics and mechanisms of dried sewage sludge, J. Hazard Mater. 160 (2008) 489–494.

[30] X. Lu, K. Shih, E. Zeng, Y.F. Wang, Effectiveness of municipal sewage sludge (MSS) ash application on the stabilization of Pb-Zn sludge from mining activities, J. Clean. Prod. 151 (2017) 145–151.

[31] S. Huang, F. Chang, S. Lo, M. Lee, C. Wang, J. Lin, Production of lightweight aggregates from mining residues, heavy metal sludge, and incinerator fly ash, J. Hazard Mater. 144 (2007) 52–55.

[32] K. You, J. Ahn, Performance of sintering process to synthesize cementitious materials and to stabilize heavy metals from MSWI fly ash and water sludge, Geosystem Eng. 15 (2012) 261–268.

[33] G. Zhen, H. Zhou, T. Zhao, Y. Zhao, Performance appraisal of controlled low-strength material using sewage sludge and refuse incineration bottom ash, Chin. J. Chem. Eng. 20 (2012) 80–88.

[34] C. Li, X. Zhang, B. Zhang, Y. Tan, F. Li, Reuse of sintered sludge from municipal sewage treatment plants for the production of lightweight aggregate building mortar, Crystals 11 (2021) 999.

[35] S. Han, Y. Song, T. Ju, Y. Meng, F. Meng, M. Song, L. Lin, M. Liu, J. Li, J. Jiang, Recycling municipal solid waste incineration fly ash in super-lightweight aggregates by sintering with clay and using SiC as bloating agent, Chemosphere 307 (2022), 135895.

[36] F. Min, X. Wang, M. Li, Y. Ni, E. Al-qadhi, J. Zhang, Preparation of high-porosity and high-strength ceramites from municipal sludge using starch and CaCO$_3$ as a combined pore-forming agent, J. Mater. Civ. Eng. 33 (2021), 04020502.

[37] G. Jia, Y. Wang, F. Yang, Z. Ma, Preparation of CFB fly ash/sewage sludge ceramsite and the morphological transformation and release properties of sulfur, Construct. Build. Mater. 373 (2023), 130864.

[38] Y. Yang, S. Shi, C. Zhu, X. Chen, Y. Hao, L. Yan, J. Li, X. Chen, B. Chen, X. Ma, Immobilization of chromium in real tannery sludge via heat treatment with coal fly ash, Chemosphere 335 (2023), 139180.

[39] G. Joseph, K. Ramamurthy, Influence of fly ash on strength and sorption characteristics of cold-bonded fly ash aggregate concrete, Construct. Build. Mater. 23 (2009) 1862–1870.

[40] W. Zatar, T. Nguyen, Mixture design study of fiber-reinforced self-compacting concrete for prefabricated street light post structures, Adv. Civ. Eng. (2020) 1–7.

[41] M. Yan, B. Prabowo, L. He, Z. Fang, Z. Xu, Y. Hu, Effect of inorganic coagulant addition under hydrothermal treatment on the dewatering performance of excess sludge with various dewatering conditions, J. Mater. Cycles Waste Manag. 19 (2016) 1279–1287.

[42] Y. Zhou, C. Liao, Z. Zhou, C. Chang, K. Shih, Effectively immobilizing lead through a melanotekite structure using low-temperature glass-ceramic sintering, Dalton Trans. 48 (2019) 3998–4006.

[43] S. Hu, S. Hu, Y. Fu, Recycling technology-Artificial lightweight aggregates synthesized from sewage sludge and its ash at lowered comelting temperature, Environ. Prog. Sustain. Energy 32 (2013) 740–748.

[44] L. Wang, G. Skjevrak, J. Hustad, O. Skreiberg, Investigation of biomass ash sintering characteristics and the effect of additives, Energy Fuel. 28 (2013) 208–218.

[45] F. Wang, X. Lu, K. Shih, C. Liu, Influence of calcium hydroxide on the fate of perfluorooctanesulfonate under thermal conditions, J. Hazard Mater. 192 (2011) 1067–1071.